

Phase separation in star polymer-colloid mixtures

J. Dzubiella,¹ A. Jusufi,¹ C. N. Likos,¹ C. von Ferber,¹ H. Löwen,¹

J. Stellbrink,^{2,3} J. Allgaier,² D. Richter,² A. B. Schofield,³ P. A. Smith,³ W. C. K. Poon,³ and P. N. Pusey³

¹ *Institut für Theoretische Physik II, Heinrich-Heine-Universität, Universitätsstraße 1, D-40225 Düsseldorf, Germany*

² *IFF-Neutronenstreuung, Forschungszentrum Jülich GmbH, D-52425 Jülich, Germany*

³ *Department of Physics and Astronomy, The University of Edinburgh, Mayfield Road, Edinburgh EH9 3JZ, United Kingdom*

(Submitted to Phys. Rev. Lett., November 17, 2018)

We examine the demixing transition in star polymer-colloid mixtures for star arm numbers $f = 2, 6, 16, 32$ and different star-colloid size ratios. Theoretically, we solve the thermodynamically self-consistent Rogers-Young integral equations for binary mixtures using three effective pair potentials obtained from direct molecular computer simulations. The numerical results show a spinodal instability. The demixing binodals are approximately calculated, and found to be consistent with experimental observations.

PACS Nos.: 61.20.-p, 61.20.Gy, 64.70.-p

The study of mixtures of hard colloidal particles and nonadsorbing polymer *chains* has received a great deal of recent attention, both experimentally [1–3] and theoretically [3–6]. However, very little is known about the phase behavior of the much richer mixture of colloidal particles and *star* polymers, the latter being macromolecules consisting of f polymeric chains covalently attached on a common center. The theoretical approaches to the study of colloid-polymer mixtures were largely based on the Asakura-Oosawa (AO) model, in which the chains are envisaged as noninteracting spheres experiencing a hard-sphere repulsion with the colloids. Subsequently, the system can be mapped onto an effective one-component fluid featuring the so-called depletion interaction between the colloids, mediated by the ideal chains [3,4]. Though the AO model provides an excellent benchmark for such systems, recent theoretical studies [5,6] and comparisons with experiments [2] indicate that the assumption of noninteracting chains leads to quantitative discrepancies between the two. Hence, a systematic effort to derive more realistic chain-chain [7] as well as chain-colloid [6,8] interactions has already been undertaken.

For the case of a star polymer-colloid mixture, the need to employ realistic interactions is even more apparent. Star polymers with a large functionality f are stiff particles [9,10] and their mutual interactions cannot be ignored, even as a first approximation. Indeed, f is the parameter which governs the softness of the star-star as well as of the star-colloid interaction, as we demonstrate below, and which provides the natural bridge between the colloid-chain mixtures (at $f = 1$ or 2) and the binary hard sphere mixture, formally equivalent to the limit $f \rightarrow \infty$. Moreover, by changing f or the degree of polymerization N of the star arms, a large domain of size ratios between the components can be covered. When the stars are of comparable size with the colloids a depletion picture of the mixture will be less accurate

than a full, two-component description because the former ignores the effects of many-body terms. In this paper, we propose analytical expressions for the star-star and star-colloid interactions for all f values and for a large range of size ratios between the two. These are based on the one hand on accurate, monomer-resolved computer simulations and on the other on theoretical arguments regarding the functional form of these interactions. Using these expressions, we make theoretical predictions on the mixing-demixing (or ‘gas-liquid’) transition in star polymer-colloid mixtures. Our measured demixing curves are in good agreement with the theoretical predictions.

We consider a binary system with N_c colloidal spheres of diameter σ_c (radius R_c) and N_s star polymers, characterized by a diameter of gyration σ_g (radius of gyration R_g) and an arm number f . For the special case $f = 2$, star polymers reduce to linear polymers and we reach the limit of colloid-polymer mixtures [1,3,4]. The total particle number is $N = N_c + N_s$. Let $q = \sigma_g/\sigma_c$ be the size ratio and $\eta_c = \frac{N_c}{V} \frac{\pi}{6} \sigma_c^3$ and $\eta_s = \frac{N_s}{V} \frac{\pi}{6} \sigma_g^3$ the packing fractions of the colloids and stars respectively, enclosed in a volume V .

Experimentally, we studied two sets of star polymer-colloid mixtures consisting of poly(methylmethacrylate) (PMMA) particles and poly(butadiene) (PB) star polymers with size ratios $q \approx 0.49$ and $q \approx 0.18$, respectively. PMMA particles were synthesized following a standard procedure [11]. Stock suspensions were prepared either in cis-decalhydronaphthalene (cis-decalin) or cis-decalin/tetrahydronaphthalene (tetralin) mixture as an index-matched solvent. These systems have been established as hard sphere models [1]. The volume fraction η_c was calibrated using the onset of the hard sphere freezing transition, taken to be at $\eta_c = 0.494$ and observed as the nucleation of iridescent colloidal crystals. The PB star polymers were prepared by anionic poly-

merization following an established procedure [12,13]. Star arms were synthesized by polymerizing butadiene with secondary butyl lithium as initiator. The resulting living polymer chains were coupled to the chlorosilane linking agent having ideally 6, 16 and 32 Si-Cl-groups. The molecular weights M_w of the PB arms were adjusted to give star polymers with values of $\langle R_g^2 \rangle^{1/2} = 0.0172 M_w^{0.609} f^{-0.403}$ [14] as close to 50 nm as possible. A linear PB polymer ($f = 2$) was prepared as a reference system. The particles and star polymers were characterized using light and small angle neutron scattering (SANS) [15]. The results are summarized in Table I.

Samples were prepared by mixing PMMA suspensions with PB stock solutions. Each sample was homogenized by prolonged tumbling and allowed to equilibrate and observed by eye at room temperature $T = 25^\circ\text{C}$ [16]. In all samples with $q \approx 0.49$, addition of polymer to suspensions with $\eta_c \sim 0.1 - 0.4$ brought about, successively, phase separation into colloidal gas and liquid (or demixing), triple coexistence of gas, liquid and crystal, and gas-crystal coexistence. In samples with $q \approx 0.18$, addition of polymer first led to fluid-crystal coexistence; a metastable gas-liquid binodal buried inside the equilibrium fluid-crystal coexistence region was encountered at higher polymer concentrations [17]. In all cases, demixing started within several hours, crystallization within two days. Here we focus on the demixing transition.

Theoretically we model the thermodynamics of the mixtures on the level of pair potentials between the two mesoscopic components, having integrated out the monomer and solvent degrees of freedom. Thus, three pair potentials are used as inputs for thermodynamically self-consistent integral equations which are closed with the Rogers-Young (RY) scheme [18]. The colloid-colloid interaction at center-to-center distance r is taken to be that of hard spheres (HS):

$$V_{cc}(r) = \begin{cases} \infty & r \leq \sigma_c; \\ 0 & \text{else.} \end{cases} \quad (1)$$

The effective interaction between two stars in a good solvent was recently derived by theoretical scaling arguments and verified by neutron scattering and molecular simulation, where the monomers were explicitly resolved [9,10]. The pair potential is modeled by an ultrasoft interaction which is logarithmic for an inner core and shows a Yukawa-type exponential decay at larger distances [9,19]:

$$V_{ss}(r) = \frac{5}{18} k_B T f^{\frac{3}{2}} \begin{cases} -\ln\left(\frac{r}{\sigma_s}\right) + \frac{1}{1+\sqrt{f/2}} & r \leq \sigma_s; \\ \frac{\sigma_s/r}{1+\sqrt{f/2}} \exp\left(-\frac{\sqrt{f}}{2\sigma_s}(r - \sigma_s)\right) & \text{else,} \end{cases} \quad (2)$$

with $k_B T$ being the thermal energy. Our computer simulations show that the so-called corona-diameter σ_s remains fixed for all considered arm numbers f , being related to the diameter of gyration through $\sigma_s \simeq 0.66\sigma_g$

[10]. However, the theoretical approach giving rise to eq. (2) does not hold for arm numbers $f \lesssim 10$, because the Daoud-Cotton model of a star [20], on which the Yukawa decay rests, is not valid for small f . In these cases, the interaction inclines to a shorter-ranged decay for $r > \sigma_s$. This is consistent with approaches in which at the linear polymer limit a Gaussian behavior of the pair potential is predicted [7,8,21]. Only the large distance decay of the interaction is affected; its form at close approaches has to remain logarithmic [22]. Accordingly, we propose the following star-star pair potential for arm numbers $f \lesssim 10$, replacing the Yukawa by a Gaussian decay:

$$V_{ss}(r) = \frac{5}{18} k_B T f^{\frac{3}{2}} \begin{cases} -\ln\left(\frac{r}{\sigma_s}\right) + \frac{1}{2\tau^2\sigma_s^2} & r \leq \sigma_s; \\ \frac{1}{2\tau^2\sigma_s^2} \exp(-\tau^2(r^2 - \sigma_s^2)) & \text{else,} \end{cases} \quad (3)$$

where $\tau(f)$ is a free parameter of the order of $1/R_g$ and is obtained by fitting to computer simulation results, see Fig. 1 and Table II. Using $\tau\sigma_s(f=2) = 1.03$ we obtain for the second virial coefficient of polymer solutions the value $B_2/R_g^3 = 5.59$, in agreement with the estimate $5.5 < B_2/R_g^3 < 5.9$ from RG and simulations [8].

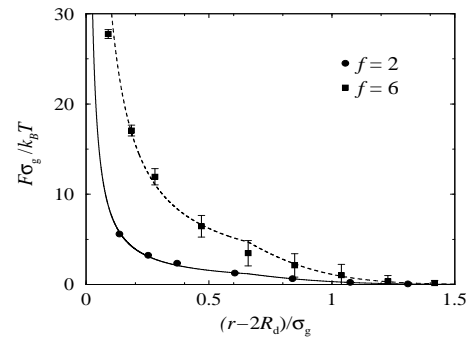


FIG. 1. Effective force between two isolated star polymers for arm numbers $f = 2, 6$ at center-to-center distance r . The theoretical result (line) derived from eq. (3) is compared to computer simulation data (symbols) to obtain the decay parameter τ . R_d is the nonvanishing core radius of one simulated star, values in Table II. Error bars are shown for the case $f = 6$ and provide an estimate for all f -values.

An analytic form for the star polymer-colloid pair potential can be found by integrating the osmotic pressure of one star along the spherical surface of a colloid, following an idea put forward by Pincus [23]. This can be achieved for arbitrary curvatures of the colloid but the analytical result below is accurate for size ratios $q \lesssim 0.7$ and reads [24]:

$$V_{sc}(r) = \Lambda k_B T f^{\frac{3}{2}} \frac{\sigma_c}{2r} \times \begin{cases} \infty & r < \frac{\sigma_c}{2}; \\ \xi_2 - \ln\left(\frac{2z}{\sigma_s}\right) - \left(\frac{4z^2}{\sigma_s^2} - 1\right)\left(\xi_1 - \frac{1}{2}\right) & \frac{\sigma_c}{2} \leq r < \frac{\sigma_s + \sigma_c}{2}; \\ \xi_2(1 - \text{erf}(2\kappa z))/(1 - \text{erf}(\kappa\sigma_s)) & \text{else,} \end{cases} \quad (4)$$

where $z = r - \sigma_c/2$ is the distance from the center of the star polymer to the surface of the colloid. The constants are $\xi_1 = 1/(1 + 2\kappa^2\sigma_s^2)$ and $\xi_2 = \frac{\sqrt{\pi}\xi_1}{\kappa\sigma_s} \exp(\kappa^2\sigma_s^2)(1 - \text{erf}(\kappa\sigma_s))$. $\Lambda(f)$ and $\kappa(f)$ are fit parameters, obtained from computer simulations where the force between an isolated star and a hard flat wall is calculated, see Fig. 2. κ is in order of $1/\sigma_g$, see the values in Table II, whereas geometrical arguments yield a limit $\Lambda_\infty = 5/36$ for very large f .

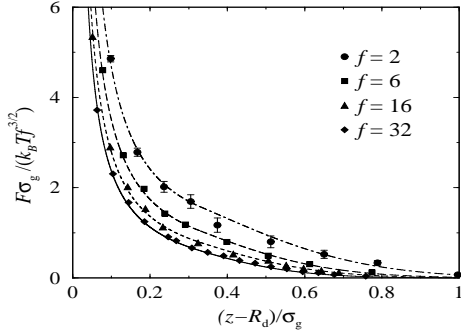


FIG. 2. Effective force between an isolated star polymer and a hard flat wall ($q = 0$) for arm numbers $f = 2, 6, 16$ and 32 . z is the distance from the star center to the surface of the wall. Theoretical curves from eq. (4) were compared to computer simulation data (symbols) to obtain the prefactor Λ and the decay parameter κ . For better comparison we divided the force by $f^{3/2}$.

To access the thermodynamics of the mixture, we solve the two-component Rogers-Young (RY) closure, which is reliable for the one component star polymer system [25] and shows spinodal instability in highly asymmetric hard sphere mixtures [26]. We also performed standard Monte Carlo (MC) simulations using the interactions (1)-(4) as inputs and measuring the structure factors at selected thermodynamics points. Excellent agreement between RY and MC was found. The thermodynamic consistency of the RY closure is enforced with a single adjustable parameter ξ ; a simple scaling of the form $\xi_{\alpha\beta} = \xi/\sigma_{\alpha\beta}$, ($\alpha, \beta = c, s$) showed only small differences compared to the unscaled form.

The structure of binary mixtures is described by three partial static structure factors $S_{\alpha\beta}(k)$, with $\alpha, \beta = c, s$ at wavevector k , obtained from the integral equations. Indication of a demixing transition is the divergence of all structure factors at the long wavelength limit $k \rightarrow 0$, marking the *spinodal line* of the system. It is more convenient to consider the concentration structure factor $S_{\text{con}}(k) = x_s^2 S_{cc}(k) + x_c^2 S_{ss}(k) - 2x_c x_s S_{cs}(k)$. We denote the partial concentrations by $x_i = N_i/N$, ($i = c, s$). The $k \rightarrow 0$ limit provides the approach to thermodynamics, through the relation [26,27]:

$$\lim_{k \rightarrow 0} S_{\text{con}}(k) = k_B T \left[\frac{\partial^2 g(x_c, P, T)}{\partial x_c^2} \right]^{-1}, \quad (5)$$

where $g(x_c, P, T)$ is the Gibbs free energy $G(x_c, N, P, T)$ per particle and P denotes the pressure of the mixture. If the function $g(x_c)$ has concave parts the system shows phase coexistence and the phase boundaries can be calculated by the common tangent construction on the $g(x_c)$ vs. x_c curves at constant P and T , ensuring the equality of the chemical potentials for each component in the two phases. The results obtained are shown in Figs. 3 and 4.

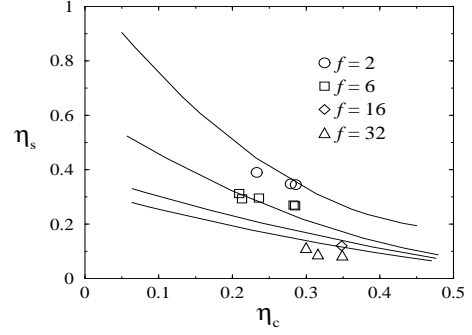


FIG. 3. Binodals for the mixing-demixing transition in star polymer-colloid mixtures for different arm numbers $f = 2, 6, 16, 32$ (from top to bottom) and size ratio $q \approx 0.49$. Symbols mark experimental results compared with theory (lines) for $q = 0.50$.

Inside the spinodal line, the limits $S_{\alpha\beta}(k \rightarrow 0)$ attain unphysical, negative values associated with the physical instability of the mixture against phase separation. Consequently, a solution of the integral equations is not possible there, and above the critical pressure P^* , $S_{\text{con}}(x_c, k = 0)$ is unknown in some interval $\Delta x_c(P)$. Thus, it is necessary to interpolate $S_{\text{con}}(x_c, k = 0)$ in order to perform the integration of eq. (5). In the vicinity of the critical point $\eta_c^* \simeq 0.3$ the missing interval Δx_c is very small and the interpolation is reliable. Here the binodals should be accurate, while for higher pressures (packing fractions $\eta_c < \eta_c^*$ and $\eta_c > \eta_c^*$) the binodals are more approximate but show reasonable behavior. For highly asymmetric systems ($q \lesssim 0.18$) it becomes more and more difficult to get solutions of the integral equations in the vicinity of the spinodal line and the calculation of binodals was not possible.

The results in Figs. 3 and 4 show that theory and experiment are in good agreement. In particular, the same trends are found as functions of the system parameters f and q . By increasing f and keeping q fixed, the demixing transition moves to lower star packing fractions η_s , as shown in Fig. 3. The largest differences occur at low arm numbers $f \lesssim 10$ which is theoretically caused by the major changes in the star-colloid pair potential for low f . When q is decreased but f remains fixed, again a motion of the binodals to lower η_s is observed, as seen in Fig. 4. This trend is *opposite* to the one predicted by the AO model [28]. The crucial parameter that determines the

trends of the phase diagram is the non-additivity of the mixture. Systems interpolating between the fully additive hard sphere mixture and the fully nonadditive AO model can feature a depletion interaction which is more attractive than in the AO limit [29]. The agreement between theory and experiment is brought about *without* the use of any free parameters in the former that would allow for a rescaling of sizes or densities. All values are read off from experiment and the only free parameters of the theory appear on the level of the pair potentials and are used only in order to fit analytical expressions to the microscopically-determined star-star and star-colloid pair interactions.

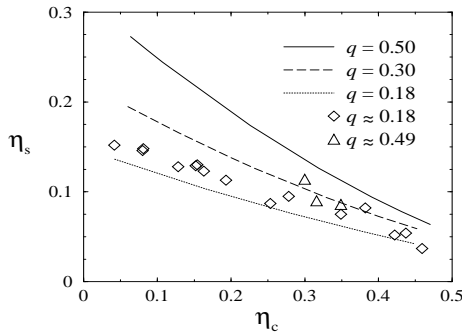


FIG. 4. Same as in Fig. 3 for an arm number $f = 32$ and different size ratios q .

To summarize, we have derived from first principles the effective interactions between the components of a star polymer-colloid mixture, proposing analytical expressions for these. We have used these to make theoretical predictions about the thermodynamic behavior of the fluid phase of the system finding very good agreement with the experimental results we obtained independently. Further work regarding, e.g., the crystallization properties of these mixtures is currently under way.

We thank M. Schmidt, A. A. Louis, R. Finken and A. Lang for useful discussions, A. Schlensog for technical support and the DFG for support within the SFB 237. J.S. is supported by the DFG and A.B.S. by NASA.

- [7] A. A. Louis *et al.*, Phys. Rev. Lett. **85**, 2522 (2000).
- [8] P. G. Bolhuis *et al.*, preprint, cond-mat/0009093.
- [9] C. N. Likos *et al.*, Phys. Rev. Lett. **80**, 4450 (1998).
- [10] A. Jusufi *et al.*, Macromolecules **32**, 4470 (1999).
- [11] L. Antl *et al.*, Coll. Surf. **17**, 67 (1986).
- [12] J. Allgaier *et al.*, Macromolecules **29**, 1794 (1996).
- [13] N. Hadjichristidis and L. J. Fetters, Macromolecules **13**, 191 (1980).
- [14] G. S. Grest *et al.*, Adv. Chem. Phys. **XCIV**, 67 (1996).
- [15] The neutron scattering was performed in *d*-cis-decalin using D11 (ILL, Grenoble, France); see *experimental report 9-11-684* (2000).
- [16] J. Stellbrink *et al.*, to be published.
- [17] W. C. K. Poon *et al.*, Faraday Discuss. **101**, 65 (1995)
- [18] F. A. Rogers and D. A. Young, Phys. Rev. A **30**, 999 (1984).
- [19] M. Watzlawek *et al.*, Phys. Rev. Lett. **82**, 5289 (1999).
- [20] M. Daoud and J. P. Cotton, J. Physique **43**, 531 (1982).
- [21] B. Krüger *et al.*, J. Phys. (Paris) **50**, 3191 (1989).
- [22] T. A. Witten and P. A. Pincus, Macromolecules **19**, 2509 (1986).
- [23] P. Pincus, Macromolecules **24**, 2912 (1991).
- [24] A. Jusufi *et al.*, to be published.
- [25] M. Watzlawek *et al.*, J. Phys.: Condens. Matter **10**, 8189 (1998).
- [26] T. Biben and J.-P. Hansen, Phys. Rev. Lett. **66**, 2215 (1991).
- [27] A. B. Bhatia and D. E. Thornton, Phys. Rev. B **2**, 3004 (1970).
- [28] M. Schmidt, private communication.
- [29] R. Roth and R. Evans, to appear in Europhys. Lett.

Monomer	f	$M_w \cdot 10^{-6} [\text{g/Mol}]^{a)}$	$R_c [\text{nm}]^{b)}$	$R_g [\text{nm}]^{a)}$
PMMA	-	-	104.0 ± 2.5	-
PMMA	-	-	289.0 ± 4.5	-
PB	2	0.57 ± 0.36	-	51.0 ± 3.5
PB	6	1.51 ± 0.06	-	52.1 ± 0.6
PB	16	3.45 ± 0.27	-	51.1 ± 0.5
PB	32	4.87 ± 0.39	-	51.4 ± 0.5

^{a)} small angle neutron scattering (SANS)

^{b)} static light scattering (SLS)

TABLE I. Molecular characteristics of PMMA particles and PB star polymers.

f	$\Lambda(f)$	$\kappa\sigma_s$	$\tau\sigma_s$	R_d/σ_g
2	0.46	0.58	1.03	0.04
6	0.35	0.71	1.16	0.03
16	0.28	0.76	-	0.04
32	0.24	0.84	-	0.06

TABLE II. Fit parameters Λ, κ, τ for the effective star-wall interaction of eq. (4) and the star-star interaction eq. (3) obtained from molecular simulation. R_d is the nonvanishing core radius of one simulated star.

- [1] S. M. Ilett *et al.*, Phys. Rev. E **51**, 1344 (1995).
- [2] A. Moussaïd *et al.*, Phys. Rev. Lett. **82**, 225 (1999).
- [3] H. N. W. Lekkerkerker *et al.*, Europhys. Lett. **20**, 559 (1992).
- [4] M. Dijkstra *et al.*, J. Phys.: Condens. Matter **11**, 10079 (1999).
- [5] A. A. Louis *et al.*, Europhys. Lett. **46**, 741 (1999).
- [6] M. Fuchs and K. S. Schweizer, Europhys. Lett. **51**, 621 (2000).